Trans. Phenom. Nano Micro Scales, 4(1): 19-28, Winter - Spring 2016
DOI: 10.7508/tpnms.2016.01.003

ORIGINAL RESEARCH PAPER

The effect of various conductivity and viscosity models considering Brownian motion on nanofluids mixed convection flow and heat transfer

H. R. Ehteram[1], A. A. Abbasian Arani[2], G. A. Sheikhzadeh[2], A. Aghaei[1,*], A. R. Malihi[3]

[1]Department of Mechanical Engineering, Mechanical Engineering University of Kashan, Kashan, I. R. Iran

Received 20 February 2015; revised 28 October 2015; accepted 21 November 2015; available online 5 January 2016

ABSTRACT: In this paper the effect of using various models for conductivity and viscosity considering Brownian motion of nanoparticles is investigated. This study is numerically conducted inside a cavity full of Water-Al_2O_3 nanofluid at the case of mixed convection heat transfer. The effect of some parameters such as the nanoparticle volume fraction, Rayleigh, Richardson and Reynolds numbers has been examined. The governing equations with specified boundary conditions has been solved using finite volume method. A computer code has been prepared for this purpose. The results are presented in form of stream functions, isotherms, Nusselt number and the flow power with and without the Brownian motion taken into consideration. The results show that for all the applied models the stream functions and isotherm have approximately same patterns and no considerable difference has been observed. In all the studied models when considering the Brownian motion, the average Nusselt number is higher than not taking this effect into account. The models of Koo-Kleinstreuer and Li-Kleinstreuer give almost same values for the maximum stream function and average Nusselt number. It is also true about the models of Vajjha-Das and Xiao et al.

KEYWORDS: *Brownian motion; Mixed convection; Nanofluid; Numerical study; Variable properties*

INTRODUCTION

Recently, nanofluids are widely used in industrial applications such as micro-turbines and micro-motors. Cooling of such systems is achieved by micro-heat exchangers, but because of their small heat transfer surface, the cooling process is not possible by ordinary fluids, so nanofluids with higher heat transfer ability than ordinary fluids can be utilized. Mansour et al. [1] numerically investigated mixed convection heat transfer in a cavity. The top lid wall was cold while the bottom wall was subjected to a constant heat flux.

Also the two side walls were at cold temperature. By their results, increment of the volume fraction of nanoparticles, reduces movement of fluid flow, but leads the Nusselt number to increase. Ghasemi and Aminossadati [2] studied mixed convection heat transfer of water-Al_2O_3 nanofluid in a right angled triangular enclosure. The horizontal wall was insulated and the vertical wall was cold while moving up or downwards. Also the inclined wall was at high temperature. They reported that in all studies Richardson numbers, Irrespective to direction of the vertical wall, increasing volume fraction of nanoparticles, enhances the heat transfer. Sheikhzadeh et al. [3] conducted numerical control
volume method to study the fluid flow and heat transfer of water-Al_2O_3 heat transfer in a cavity. The horizontal walls were adiabatic which the top one was moving. Right and left walls were considered at high and low constant temperature, respectively. They found that considering variable conductivity and viscosity for nanofluid leads to different values of Nusselt number in comparison with those of constant properties. Withal, their report show that in low Richardson numbers (0.01 & 0.1) this difference is more obvious than high Richardson numbers (10, 100). Pishkar and Ghasemi [4] numerically investigated flow and heat transfer of Water-Cu nanofluid in a finned horizontal canal. Their results show that by increasing the nanoparticle volume fraction and Reynolds number, the heat transfer enhances. For a fixed volume fraction, this enhancement is much better at higher Reynolds numbers. Chamkhaa and Abu-Nada [5] examined nanofluid flow and heat transfer in a cavity with adiabatic vertical walls, while the top and bottom side of cavity were at high and low temperature respectively. They considered two different cases for movement of horizontal walls. In first case, only the top wall was moving while in second case both of bottom and top walls were moving in opposite directions. Their results show augmentation of the Nusselt number by increment of the nanoparticle volume fraction and decrement of the Richardson number. Abbasian et al. [6] implemented a numerical study of flow and heat transfer of water-Cu nano-

*Corresponding Author Email: *alirezaaghaei21@gmail.com*
Tel.: +989135535460

Nomenclature

c_p	specific heat ($Jkg^{-1}K^{-1}$)
d	diameter (nm)
Gr	grashof number
g	gravitational acceleration ($m.s^{-2}$)
H	height of the enclosure (m)
k	thermal conductivity ($Wm^{-1}K^{-1}$)
Nu	Nusselt number
p	pressure ($kg\ m^{-1}s^{-2}$)
P	dimensionless pressure
Ra	Rayleigh number
Ri	Richardson number
Re	Reynolds number
Pr	Prandtl number
T	temperature (K)
u, v	dimensional x and y components of velocity
U,V	dimensionless velocities
U0	reference velocity
x, y	dimensional coordinates
X, Y	dimensionless coordinate

Greek Symbols

α	thermal diffusivity (m^2s^{-1})
β	thermal expansion coefficient (K^{-1})
μ	dynamic viscosity ($kgm^{-2}s^{-1}$)
ν	kinematic viscosity (m^2s^{-1})
θ	dimensionless temperature
ρ	density (kgm^{-3})
ϕ	nanoparticle volume fraction
ψ	stream function
Ψ	dimensionless stream function

Subscripts

avg	average
c	cold
cp-p	particle
eff	effective
f	fluid
h	hot
nf	nanofluid
p	particle
0	reference conditions

fluid in a cavity which its lateral walls were subjected to a sinusoidal temperature distribution and the horizontal walls were insulated. They reported that in a fixed Richardson number and volume fraction of nanoparticles, by increment of the phase difference, the heat transfer augments.

Here we present a summary of previous studies on Brownian motion. Ghasemi and Aminossadati [7] conducted a numerical study on natural convection of Water-CuO in a triangular enclosure. The inclined wall was cold and two other walls were adiabatic except the central part of the vertical wall which was considered at high temperature. They showed that with the Brownian motion of nanoparticles taken into account, the volumetric fraction of solid nanoparticles has different effects on heat transfer in various Rayleigh numbers. In low Rayleigh numbers considering Brownian motion of nanoparticles, increasing volume fraction leads to a notable increase in Nusselt number whereas this increment is lesser when not considering Brownian effects. In high Rayleigh numbers when considering Brownian motion of nanoparticles, increment in Nusselt number with increasing volume fraction is not significant in comparison with low Rayleigh numbers. By their results, in high Rayleigh numbers there is an optimal value for volumetric fraction of nanoparticles in which maximum heat transfer is achieved. Pakravan and Yaghoubi [8] studied the dufour effect, thermophoresis and Brownian motion in natural convection of Water-Al_2O_3, Water-CuO, Water-TiO_2 nanofluids. According to their results, simultaneous effect of these mechanisms on Nusselt number is highly depended on considered geometry. They reported increment of the average Nusselt number by increasing volume fraction of nanoparticles in cavity. Wang et al. [9] numerically studied mixed convection flow and heat transfer of Water-CuO nanofluid in a cavity. Horizontal walls were insulated while the left and right wall were hot and cold respectively. They observed that with the Brownian effects taken into account, the Nusselt number shows more increment with increasing volumetric fraction of solid particles. Whereas in Richardson number of 0.01 and volume fraction of 0.04, the computed average Nusselt number when considering the Brownian motion of nanoparticles was 4% greater than that of forbearing the Brownian effects. Haddad et al. [10] observed the effects of thermophoresis and Brownian motion in natural convection heat transfer. They conducted their study on Water-CuO nanofluid inside a cavity which its bottom and top walls were at high and low temperature respectively. Theirs results showed an augmentation in heat transfer rate when considering thermophoresis and Brownian effects for all the studied volume fractions and this increment was much greater in low solid concentrations. Seyf and Nikaaein [11] investigated forced convection heat transfer of ethylene-Glycol based nanofluids in a microchannel heat sink (MCHS) with CuO, Al_2O_3 and ZnO as nanoparticles. Based on their observations, the effect of Brownian motion was more significant for smaller nanoparticles. Abbasian et al. [12] studied Brownian motion of nanoparticles in mixed convection of Water-CuO nanofluid in a cavity containing an inside square heater, while all of the cavity walls were cold. By their results, the average Nusselt number rise with increasing Richardson number whether considering Brownian effects or not.

Also they reported that when the Brownian motion of nanoparticles is taken into account, the resulting average Nusselt numbers are greater than those of not considering the Brownian effects.

This paper is concerned with investigation of the effect of considering different models for Brownian motion on

mixed convection flow and heat transfer of Water-Al_2O_3 nanofluid inside a cavity. Effect of various parameters such as the nanoparticle volume fraction, Rayleigh, Richardson and Reynolds numbers are also studied. A constant Grashof number $Gr=10^4$ was considered. Richardson number and volume fraction of nanoparticles were considered in range of $0.01< Ri <100$ and $0< \phi <4\%$ respectively. The results are presented with and without the Brownian effects taken into account.

GOVERNING EQUATIONS AND BOUNDARY CONDITIONS

The geometry of problem and boundary conditions is shown in Figure 1. Horizontal walls of the cavity are insulated while the left and right walls are at high and low temperatures respectively (T_h and T_c). The enclosure has a length of H. the Thermophysical properties of water as the base fluid and alumina nanoparticles are presented in table 1 [13].

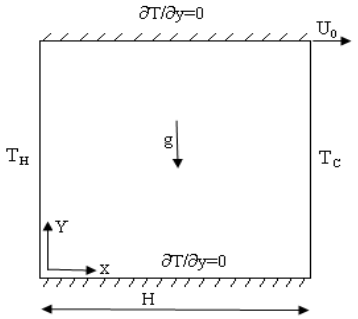

Fig. 1. Schematic of the enclosure

Table 1
Thermo-physical properties of base fluid and nanoparticles [13].

	ρ (kgm^{-3})	c_p ($jkg^{-1}K^{-1}$)	k ($Wm^{-1}K^{-1}$)	β (K^{-1})
Water	997.1	4179	0.613	$10^{-4}\times2.1$
Al_2O_3	3970	765	40	$10^{-5}\times0.85$

The equations of continuity, momentum in both directions, energy and the relation of stream function can be written as follows [14].

$$\frac{\partial(\rho_{nf}u)}{\partial x}+\frac{\partial(\rho_{nf}v)}{\partial y}=0 \tag{1}$$

$$\frac{\partial}{\partial x}(\rho_{\mathrm{nf}}uu)+\frac{\partial}{\partial y}(\rho_{\mathrm{nf}}vu)=\frac{\partial p}{\partial x}+\frac{\partial}{\partial x}(\mu_{\mathrm{nf}}\frac{\partial u}{\partial x})+\frac{\partial}{\partial y}(\mu_{\mathrm{nf}}\frac{\partial u}{\partial y}) \tag{2}$$

$$\frac{\partial}{\partial x}(\rho_{\mathrm{nf}}vu)+\frac{\partial}{\partial y}(\rho_{\mathrm{nf}}vv)=\frac{\partial p}{\partial y}+\frac{\partial}{\partial x}(\mu_{\mathrm{nf}}\frac{\partial v}{\partial x})+\frac{\partial}{\partial y}(\mu_{\mathrm{nf}}\frac{\partial v}{\partial y}) +(\rho\beta)_{\mathrm{nf}}\mathrm{g}(T-T_c) \tag{3}$$

$$\frac{\partial}{\partial x}(\rho_{nf}c_{nf}uT)+\frac{\partial}{\partial y}(\rho_{nf}c_{nf}vT)=\frac{\partial}{\partial x}(k_{\mathrm{nf}}\frac{\partial T}{\partial x})+\frac{\partial}{\partial y}(k_{\mathrm{nf}}\frac{\partial T}{\partial y}) \tag{4}$$

$$\psi(\mathrm{x,y})=\int\rho_{\mathrm{nf}}udy+\psi_0 \tag{5}$$

Using the dimensionless parameters of (6), the non-dimensional equations including continuity (7), momentum in both directions (8, 9) and energy (10) for laminar, two dimensional and steady flow are achieved:

$$X=\frac{x}{H},Y=\frac{y}{H},U=\frac{u}{U_0},V=\frac{v}{U_0}$$

$$\rho^*=\frac{\rho_{nf}}{\rho_{f,0}},\beta^*=\frac{\beta_{nf}}{\beta_{f,0}},\mu^*=\frac{\mu_{nf}}{\mu_{f,0}},c^*=\frac{c_{nf}}{c_{f,0}}$$
$$\theta=\frac{T-T_c}{T_h-T_c},P=\frac{p}{\rho_{f,0}U_0^{\ 2}},Re=\frac{\rho_{f,0}U_0H}{\mu_{f,0}} \tag{6}$$
$$Ri=\frac{Gr}{\mathrm{Re}^2},Gr=\frac{g\beta\Delta TH^3}{\upsilon_{f,0}^2},Pr=\frac{\upsilon_{f,0}}{\alpha_{f,0}}$$

$$\frac{\partial(\rho^*U)}{\partial X}+\frac{\partial(\rho^*V)}{\partial Y}=0 \tag{7}$$

$$\frac{\partial}{\partial X}(\rho^*UU)+\frac{\partial}{\partial Y}(\rho^*VU)=-\frac{\partial P}{\partial X}+\frac{1}{Re}[\frac{\partial}{\partial X}\left(\mu^*\frac{\partial U}{\partial X}\right)+\frac{\partial}{\partial Y}\left(\mu^*\frac{\partial U}{\partial Y}\right)] \tag{8}$$

$$\frac{\partial}{\partial X}(\rho^*UV)+\frac{\partial}{\partial Y}(\rho^*VV)=-\frac{\partial P}{\partial Y}+\frac{1}{Re}[\frac{\partial}{\partial X}\left(\mu^*\frac{\partial U}{\partial X}\right)+\frac{\partial}{\partial Y}\left(\mu^*\frac{\partial U}{\partial Y}\right)]+Ri\rho^*\beta^*\theta \tag{9}$$

$$\frac{\partial}{\partial X}(\rho^*c^*U\theta)+\frac{\partial}{\partial Y}(\rho^*c^*V\theta)=\frac{1}{Re\ Pr}[\frac{\partial}{\partial X}\left(k^*\frac{\partial\theta}{\partial X}\right)+\frac{\partial}{\partial Y}\left(k^*\frac{\partial\theta}{\partial Y}\right)] \tag{10}$$

Also the dimensionless stream function is determined by:

$$\Psi(X,Y)=\int\rho^*UdY+\Psi_0 \tag{11}$$

According to geometry of the problem, the dimensionless boundary conditions are:

$$\begin{aligned}
&U=1,\ V=0,\ \frac{\partial\theta}{\partial Y}=0 && \text{Top wall}\\
&U=V=0,\ \frac{\partial\theta}{\partial Y}=0 && \text{Bottom wall}\\
&U=0,\ V=0,\ \theta=0 && \text{Right wall}\\
&U=0,\ V=0,\ \theta=1 && \text{left wall}
\end{aligned} \tag{12}$$

The nanofluid properties including density, heat capacitance, thermal expansion coefficient [15], diffusivity,

static viscosity [16] and static conductivity [17] are respectively determined by equations (13) to (18):

$$\rho_{nf} = 1001.064 + 2738.6191\phi - 0.2095T \quad (13)$$

$$(\rho c_p)_{nf} = (1-\phi)(\rho c_p)_f + \phi(\rho c_p)_s \quad (14)$$

$$\beta_{nf} = (-0.479\phi + 9.3158\times10^{-3}T - \frac{4.7211}{T^2})\times10^{-3} \quad (15)$$

$$\alpha_{nf} = \frac{k_{nf}}{(\rho c_P)_{nf}} \quad (16)$$

$$\mu_{Static} = \mu_f(1-\phi)^{-2.5} \quad (17)$$

$$k_{Static} = k_f\left[\frac{(k_s+2k_f)-2\phi(k_f-k_s)}{(k_s+2k_f)+\phi(k_f-k_s)}\right] \quad (18)$$

Viscosity and conductivity considering the Brownian motion of nanoparticles are calculated by equations 19 and 20. $\mu_{Brownian}$ and $K_{Brownian}$ are distinctly calculated in different models.

$$\mu_{nf} = \mu_{Static} + \mu_{Brownian} \quad (19)$$

$$k_{nf} = k_{Static} + k_{Brownian} \quad (20)$$

$K_{Brownian}$ of the model of Koo and Kleinstreuer is [18]:

$$k_{Brownian} = 5\times10^4\lambda\phi\rho_f c_{p,f}\sqrt{\frac{\kappa T}{\rho_p d_p}}\xi(T,\phi) \quad (21)$$

ρ_p and d_p are the nanoparticle's density and diameter respectively. For the Water-Al_2O_3 nanofluid, the correlations of λ and ζ for the range of 300<*T* (K) <325 are [18]:

$$\lambda = 0.0017(100\phi)^{-0.0841} \quad \text{for} \quad \phi > 1\% \quad (22)$$

$$\xi(T,\varphi) = (-6.04\varphi + 0.4705)T + (1722.3\varphi - 134.63) \quad \text{for} \quad 1\% < \phi < 4\% \quad (23)$$

In Vajjha-Das model, $K_{Brownian}$ is also determined by [21].
The functions ζ and λ for this model at range of 298<*T* (K) <363 are determined as followed [19]:

$$\xi(T,\varphi) = (2.8217\times10^{-2}\varphi + 3.917\times10^{-3})\frac{T}{T_0} + (-3.0669\times10^{-2}\varphi - 3.91123\times10^{-3}) \quad (24)$$

$$\lambda = 8.4407(100\phi)^{-1.07304} \quad for \quad 1\% < \phi < 10\% \quad (25)$$

K is the Boltzmann constant ($K=1.3807\times10^{-23}J/K$). In model of Li-Kleinstreuer $K_{Brownian}$ is [20]:

$$k_{Brownian} = 5\times10^4\phi\rho_f c_{p,f}\sqrt{\frac{\kappa T}{\rho_p d_p}}f(T,\phi) \quad (26)$$

For Water-Al_2O_3 nanofluid, the correlation of *f* is written as [20]:

$$f = (a + b\ln(d_p) + c\ln(\phi) + d\ln(\phi)\ln(d_p) + e\ln(d_p)^2)\ln(T) + (g + h\ln(dp) + i\ln(\phi) + j\ln(\phi)\ln(d_p) + k\ln(d_p)^2) \quad (27)$$

The constants of (27) for Water-Al_2O_3 nanofluid is given in table 2 [20].

Table 2
Constants of (27) for Water-Al_2O_3 nanofluid [20].

Const.	Value	Const.	Value
g	-298.1981	*a*	52.8135
h	-34.5327	*b*	6.1156
i	-3.92253	*c*	0.6956
j	-0.2354	*d*	0.0417
k	-0.9991	*e*	0.1769

$K_{Brownian}$ in model of Xiao et al. is [21]:

$$k_{Brownian} = \frac{CD_f k_f\left[\frac{3}{\alpha}\sqrt{\frac{2k_bT}{\pi\rho_p}}\frac{(K^{\frac{1}{2-d_f}}-1)d_f^{1/8}}{2d_f-1} + \frac{2(K^{1-d_f}-1)(4-d_f)^{1/8}D_{av}^{1/2}}{d_f-1}\right]}{Pr(1-K^{2-d_f})(4-d_f)^{3/8}(2-d_f)^{-1}d_f^{1/4}D_p^{3/2}} \quad (28)$$

In this relation the fractal dimension (d_f) and *K* are given as follows:

$$d_f = 2 - \frac{\ln\phi}{\ln10^{-3}} \quad (29)$$

$$k = \frac{D_{min}}{D_{max}} \quad (30)$$

In this study $D_f = 0.384\times10^{-9}$ (the diameter of base fluid), $k = 10^{-3}$ and $c = 236\times10^{-3}$ [21]. In all of the foresaid models, $\mu_{Brownian}$ is determined by [18]:

$$\mu_{Brownian} = \frac{k_{Brownian}}{k_f}\times\frac{\mu_f}{Pr} \quad (31)$$

The heat transfer coefficient is computed from:

$$h_{nf} = \frac{q}{T_h - T_c} \quad (32)$$

The Nusselt number which its characteristic length is equal to the cavity height, can be expressed as:

$$\mathrm{Nu}=\frac{h_{nf}\mathrm{H}}{k_f} \tag{33}$$

Heat flux per unit area of the cavity walls can be calculated from:

$$q=-k_{nf}\frac{T_h-T_c}{H}\frac{\partial\theta}{\partial X}\bigg|_{X=0} \tag{34}$$

Substituting relations (32) and (34) in (33), gives the Nusselt number:

$$\mathrm{Nu}=-\left(\frac{k_{nf}}{k_f}\right)\frac{\partial\theta}{\partial X}\bigg|_{x=0} \tag{35}$$

The average Nusselt number on the hot wall is determined from:

$$\mathrm{Nu}_{\mathrm{Avg}}=\int_0^1 Nu \quad dY \tag{36}$$

NUMERICAL METHOD

The governing equations are solved by finite volume numerical method and the SIMPLER algorithm. In order to validate the results of the computer code, a numerical simulation is performed and the results are compared with [5] in Table 3.

Table 3
Average Nusselt number validation for different Richardson numbers and volume fractions.

Ri	ϕ	Present work	Reference [5]	Relative difference (%)
0.001	0	32.33	32.39	0.19
	0.05	34.35	34.42	0.20
	0.1	36.40	36.90	1.36
1	0	4.62	4.73	2.33
	0.05	4.71	4.83	2.48
	0.1	4.79	4.94	3.04
10	0	1.63	1.68	2.98
	0.05	1.75	1.82	3.85
	0.1	1.87	1.95	4.10

In order to determine a proper grid for the numerical simulations, a grid independence test is conducted for the problem of mixed convection heat transfer of Water-Al_2O_3 nanofluid.

A non-uniform grid with an expansion ratio of 1.05 has been chosen and the average Nusselt number is carried out and compared for different grid sizes. According to the Nusselt number values presented in Table 4, this is clear that a mesh with 81× 81 points is good enough to ensure a mesh independent solution. Hence, this grid is used for the present study.

The convergence criteria for pressure, velocity and temperature is written as (37). Where m and n are the number of grid points on *x*- and *y*-directions, respectively, *k* is any of the computed field variables. ε is the iteration number and the maximum error is set to 10^{-7}.

$$\mathrm{Error}=\frac{\sum_{i=1}^{M}\sum_{j=1}^{N}\left|\epsilon_{i,j}^{k+1}-\epsilon_{i,j}^{k}\right|}{\sum_{i=1}^{M}\sum_{j=1}^{N}\left|\epsilon_{i,j}^{k+1}\right|}\le 10^{-7} \tag{37}$$

RESULTS

Velocity and temperature fields

In Figure 2 and 3, the variations of velocity magnitude and temperature at the central line is plotted for nanoparticle volume fraction of 0.04 and Richardson numbers of 0.01 and 100.

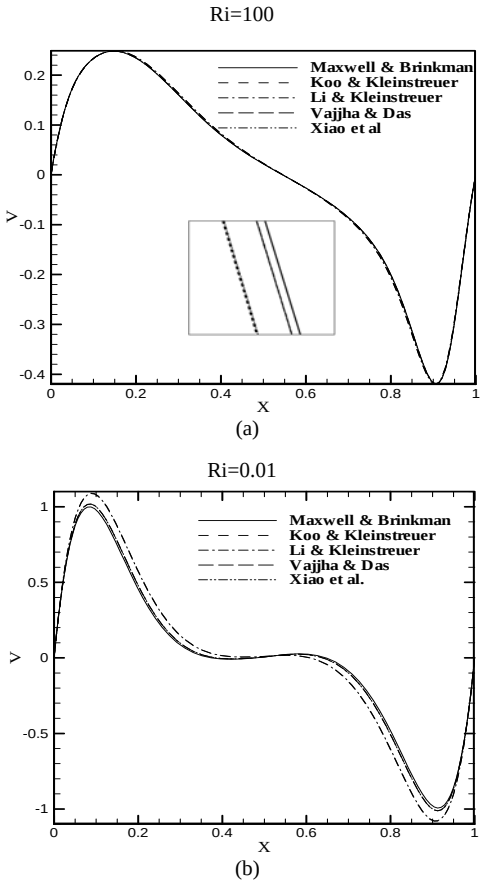

Fig. 2. Comparison of velocity variations at the horizontal mid-section in terms of X for all models ϕ =0.04

Maximum stream function

At Table 5 the maximum stream function due to mixed convection derived from various models is presented. For all the applied models with increasing nanoparticle volume fraction the maximum stream function increase, as a measure of the flow strength. In mixed convection, the flow is more affected from the lid velocity, so the increment of viscosity arising from the increasing volume fraction can't

overcome the added power to flow because of the lid velocity and increasing conductivity (arising from the increasing volume fraction).

Consequently, the flow power augments. In all of the studied models, the flow power augments with increasing Richardson number up to 1 and after that turns to decrease. This is in contrast with Table 5 and this contradiction is because of the difference in the way that velocity and stream function are non-dimensioned.

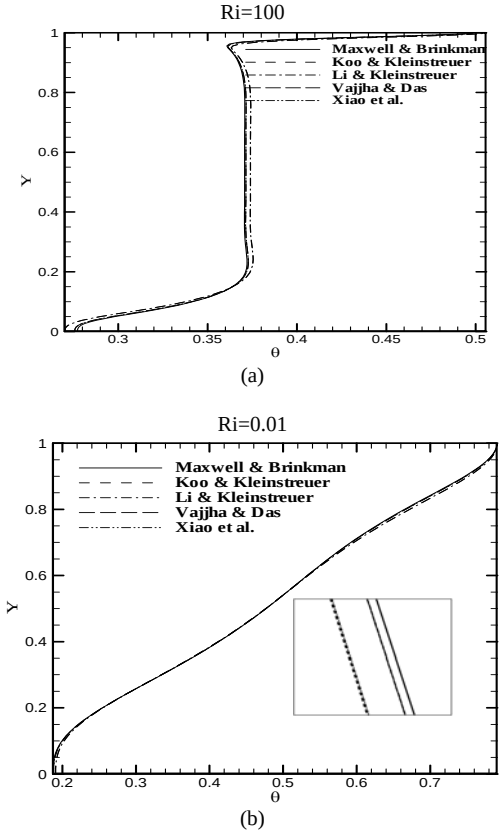

Fig. 3. Comparison of Temperature variations at the horizontal mid-section in terms of X for all models ϕ =0.04

Increment of the Richardson number shows the augmentation of natural convection against forced convection and consequently a decrease in the power of vortexes.

With this in mind, the variations of flow power is justifiable.

For all the studied models and at all Richardson numbers, the most increment of the stream function maximum value with the increase in nanoparticle volume fraction from 0 up to 0.04 is equal to 39.78 percent. When applying the model of Koo-Kleinstreuer, this is happened at Richardson number of 100.

Also with increasing volume fraction of the nanoparticles, the least increment in maximum stream function is equal to 10.82 and is due to the model of Maxwell-Brinkman and Richardson number of 0.01.

Table 5
Results for maximum stream function due to (a) Maxwell-Brinkman, (b) Koo-Kleinstreuer, (c) Li-Kleinstreuer, (d) Vajjha-Das and (e) Xiao et al. models.

(a)

Ri	ϕ =0	ϕ =0.04
0.01	0.0777	0.0861
0.1	0.1006	0.1116
1	0.1037	0.1152
10	0.0979	0.1110
100	0.1674	0.2005

(b)

Ri	ϕ =0	ϕ =0.04
0.01	0.0777	0.0873
0.1	0.1006	0.1121
1	0.1037	0.1155
10	0.0979	0.1146
100	0.1674	0.2340

(c)

Ri	ϕ =0	ϕ =0.04
0.01	0.0777	0.0872
0.1	0.1006	0.1121
1	0.1037	0.1155
10	0.0979	0.1147
100	0.1674	0.2329

(d)

Ri	ϕ =0	ϕ =0.04
0.01	0.0777	0.0863
0.1	0.1006	0.1117
1	0.1037	0.1153
10	0.0979	0.1121
100	0.1674	0.2071

(e)

Ri	ϕ =0	ϕ =0.04
0.01	0.0777	0.0863
0.1	0.1006	0.1117
1	0.1037	0.1153
10	0.0979	0.1121
100	0.1674	0.2071

Average Nusselt number

In Figure 5The variations of average Nusselt number in mixed convection heat transfer applying various models at different Richardson numbers in terms of volume fraction of nanoparticles are presented. In all of the studied models and at all Richardson numbers, the average Nusselt number augments with increasing volume fraction. For all Richardson numbers, the results derived by using models of Koo-Kleinstreuer and Li-Kleinstreuer show the most increment in Nusselt number with increasing volume fraction.

In mixed convection heat transfer, the flow power is more affected by the lid velocity than the predicted viscosity by various applied models. It shows that in mixed convection heat transfer, the effect of change in conductivity due to using various models is more important

than the effect of change in viscosity. These two models show the most increment in conductivity among all models, so more increase in Nusselt number when applying these models is acceptable.

At all Rayleigh numbers in nanoparticle volume fraction of 0.04, the models of Koo-Kleinstreuer and Li-Kleinstreuer estimate same values for average Nusselt number. This condition also apply to Vajjha-Das and Xiao et al. models.

Also from Table 5 it is clear that the maximum stream function values are very close to each other for all nanoparticle volume fractions. From the two above-mentioned items, the behavior of the aforementioned models at the volume fraction of 0.04 is justifiable.

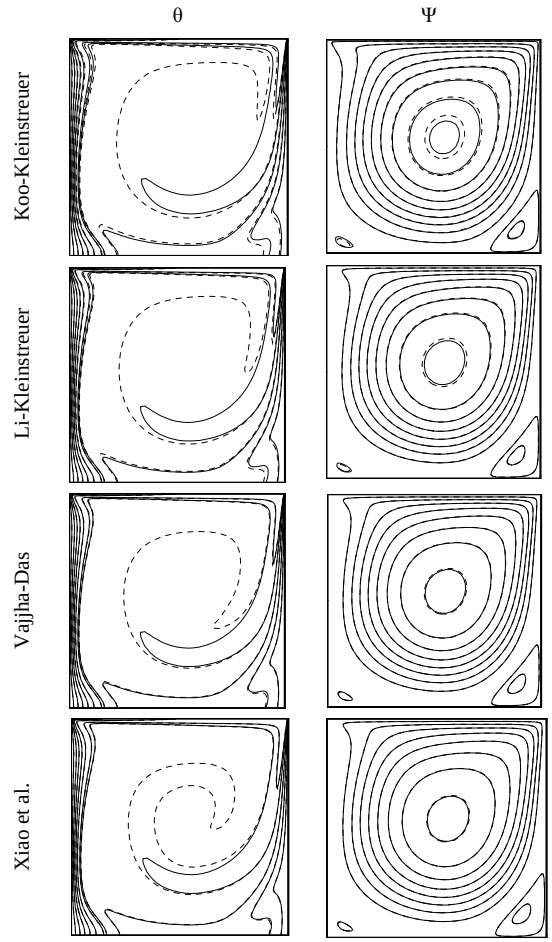

Fig. 4. Comparison between the Stream functions and isotherms due to various models with the model of Maxwell-Brinkman at Ri=0.01, ϕ =0.02

For instance, the values of average Nusselt number applying the model of Koo-Kleinstreuer at various Rayleigh numbers and nanoparticle volume fractions is presented in Table 6. And is compared with those of Maxwell-Brinkman's model. The most and least increment in average Nusselt number when the Brownian motion of nanoparticles is taken into account compared to those of not considering this effect is 17.68% and (at Richardson number of 0.01 for nanoparticle volume fraction of 0.03) and 14.84 (at Richardson number of 100 for nanoparticle volume fraction of 0.02) respectively.

In order to investigate accuracy and validation of the models used in this article, this models had been compared with an experimental and special model of water-Al_2O_3 nanofluid [22]. In figure 5 the values of the average Nusselt numbers had been shown for this model. With attention to the values of the average Nusselt numbers it can be concluded that through investigated models in this article, the Koo-Kleinstreuer model has the closest behavior to experimental model. The maximum difference in values of the average Nusselt numbers predicted by this model with the experimental model is about % 6. Also The results indicate that in low Ri numbers the difference between the values of the average Nusselt numbers in the investigated models with the experimental model reduce (in comparison with higher Ri).

CONCLUSIONS

In this numerical study, the effect of various Brownian models on mixed convection flow and heat transfer of Water-Al_2O_3 nanofluid inside a cavity at constant grashof number of 10^4, a range of 0.1-100 for Richardson number and ϕ =0, 0.02, 0.03 and 0.04 is investigated. The results are presented with and without taking the Brownian effects into consideration. Here is an overview of the results carried out in previous chapters.

1) For all of the studied models, the streamlines and isotherms have similar behavior and no significant difference was seen.
2) For all of the studied models, the calculated average Nusselt number when considering the Brownian motion of nanoparticles is higher than that of not taking the Brownian effects into account.
3) The models of Koo-Kleinstreuer and Li-Kleinstreuer predict almost the same values for maximum stream function and average Nusselt number. This is also true for Vajjha-Das and Xiao et al. models.
4) For all of the applied models, with increasing Richardson number, the flow power decreases until Richardson of 1 and then rise until Richardson of 10 and after that, again turns to decrease. The most increment in maximum stream function with increasing nanoparticle volume fraction from 0 up to 0.04 is equal to 39.78% and is taken effect at Richardson number of 100 by applying the model of Koo-Kleinstreuer. Also the least increment in maximum stream function is equal to 10.82 and is due to Richardson number of 0.01 by applying Maxwell brinkman model.
5) For all of the applied models, the maximum stream function as a measure of the flow power; rise with increasing nanoparticle volume fraction.

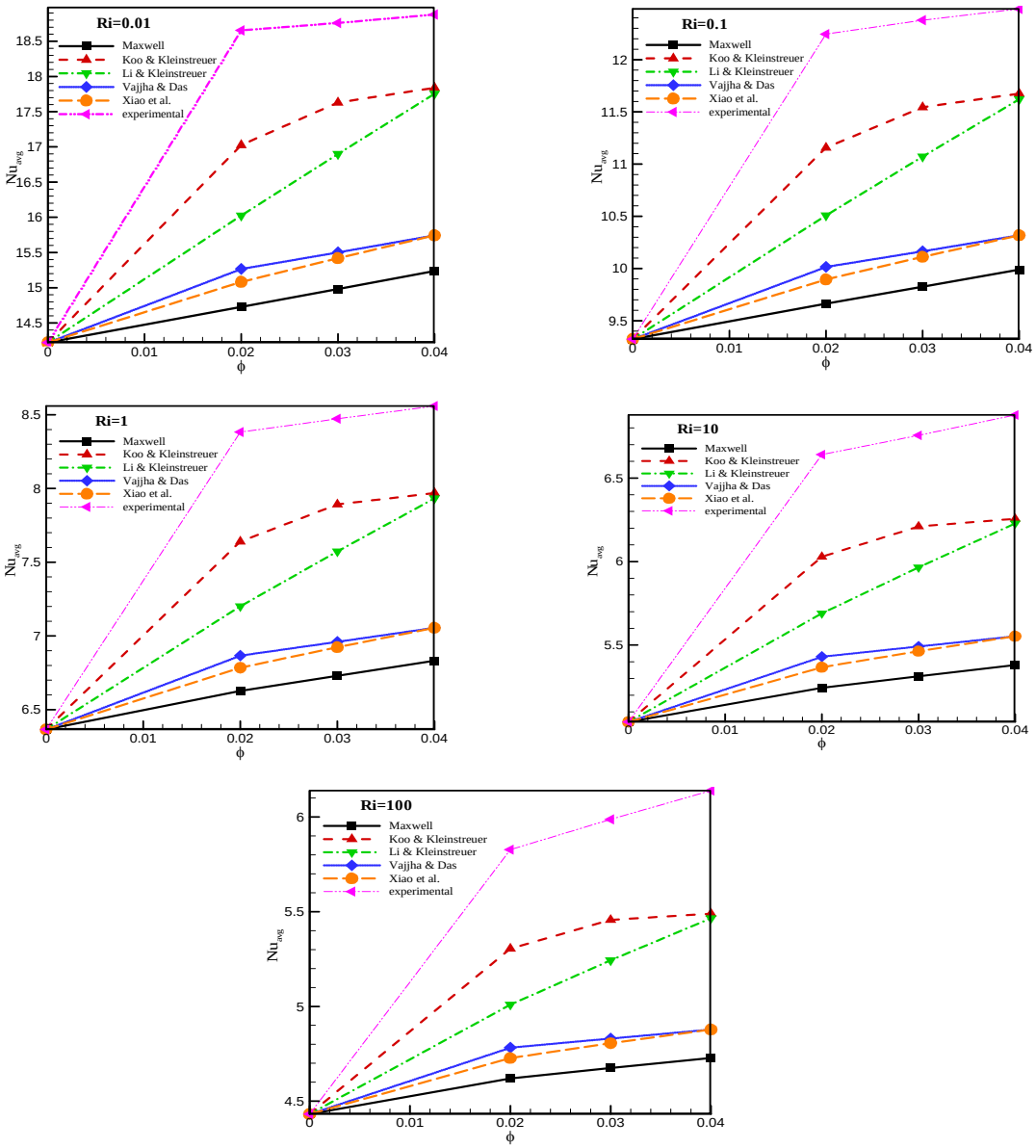

Fig. 5. Variations of the average Nusselt number of the hot wall with respect to ϕ for different values of Ri

6) For all models at all Richardson numbers, the average Nusselt number augments with increasing volume fraction of nanoparticles.
7) The most and least increment in computed average Nusselt numbers when the Brownian motion of nanoparticles is taken into account compared to those of not considering this effect was 17.68% (at Richardson number of 0.01 for nanoparticle volume fraction of 0.03) and 14.84 (at Richardson number of 100 for nanoparticle volume fraction of 0.02) respectively.
8) The more the applied model is dependent to the temperature variations, the more this dependency is obvious in low Richardson numbers. Increasing Richardson number leads the temperature variations with respect to Y to be linear.
9) With attention to the values of the average Nusselt numbers it can be concluded that through investigatedmodels in this article, the Koo-Kleinstreuer model has the closest behavior to experimental model.

Table 6
Comparison of average Nusselt number values due to models of Koo-Kleinstreuer and MaxwellBrinkman for various nanoparticle volume- fractions and Richardson numbers.

Ri	model	ϕ =0	ϕ =0.02	ϕ =0.03	ϕ =0.04
0.01	Maxwell-Brinkman	14.2212	14.7268	14.9813	15.2375
	Koo-Kleinstreuer	14.2212	17.0254	17.6304	17.8391
	Relative Increment (%)	0	15.61	17.68	17.07
0.1	Maxwell-Brinkman	9.3241	9.6633	9.8259	9.9889
	Koo-Kleinstreuer	9.3241	11.1571	11.5446	11.6752
	Relative Increment (%)	0	15.46	17.49	16.88
1	Maxwell-Brinkman	6.3660	6.6269	6.7295	6.8318
	Koo-Kleinstreuer	6.3660	7.6402	7.8919	7.9694
	Relative Increment (%)	0	15.29	17.27	16.65
10	Maxwell-Brinkman	5.0398	5.2443	5.3131	5.3803
	Koo-Kleinstreuer	5.0398	6.0289	6.2103	6.2564
	Relative Increment (%)	00	14.96	16.89	16.28
100	Maxwell-Brinkman	4.4316	4.6196	4.6845	4.7274
	Koo-Kleinstreuer	4.4316	5.3051	5.4568	5.4899
	Relative Increment (%)	0	14.84	16.74	16.13

REFERENCES

[1] M.A. Mansour, R.A. Mohamed, M.M. Abd-Elaziz, S.E. Ahmed: Numerical simulation of mixed convection flows in a square lid-driven cavity partially heated from below using nanofluid, International Communications in Heat and Mass Transfer 37 (2010) 1504–1512.

[2] B. Ghasemi, S.M. Aminossadati: Mixed convection in a lid-driven triangular enclosure filled with nanofluids, International Communications in Heat and Mass Transfer 37 (2010) 1142–1148.

[3] G.A. Sheikhzadeh, M. Ebrahim Qomi, N. Hajialigol, A. Fattahi: Numerical study of mixed convection flows in a lid-driven enclosure filled With nanofluid using variable properties, International Results in Physics 2 (2012) 5-13.

[4] I. Pishkar, B. Ghasemi: Cooling enhancement of two fins in a horizontal channel by nanofluid mixed convection, International Journal of Thermal Sciences 59 (2012) 141-151.

[5] A. J. Chamkhaa, E. Abu-Nada: Mixed convection flow in single- and double-lid driven square cavities filled with water–Al_2O_3 nanofluid: Effect of viscosity models, European Journal of Mechanics B/Fluids 36 (2012) 82-96.

[6] A.A. Abbasian Arani, S. Mazrouei Sebdani, M. Mahmoodi, A. Ardeshiri, M. Aliakbari: Numerical study of mixed convection flow in a lid-driven cavity with sinusoidal heating on side walls using nanofluid, Super lattices and Micro structures 51 (2012) 893-911.

[7] B. Ghasemi, S.M. Aminossadati: Brownian motion of nanoparticles in a triangular enclosure with natural convection, International Journal of Thermal Sciences 49 (2010) 931–940.

[8] H.A. Pakravan, M. Yaghoubi: Combined thermophoresis, Brownian motion and Dufour effec ts on natural convection of nano fluids, International Journal of Thermal Sciences 50 (2011) 394 – 402.

[9] X. Wang, D. Li, H. Jiao: Heat Transfer Enhancement of CuO-water Nanouids Considering Brownian Motion of Nanoparticles in a Singular Cavity, Journal of Information & Computational Science 9 (2012) 1223-1235.

[10] Z. Haddad, E. Abu-Nada, H.F. Oztop, A. Mataoui: Natural convection in nanofluids: Are the thermophoresis and Brownian motion effects significant in nano fluid heat transfer enhancement?, International Journal of Thermal Sciences 57 (2012) 152 -162.

[11] H.R. Seyf, B. Nikaaein: Analysis of Brownian motion and particle size effects on the thermal behavior and cooling performance of microchannel heat sinks, International Journal of Thermal Sciences 58 (2012) 36-44.

[12] A. A. Abbasian Arani, A. Aghaei, H. Ehteram: Numerical investigation of Brownian motion effect on nanofluid mixed convection in enclosure with a hot central heat source, Journal of Modeling in Engineering Semnan University (2013).

[13] E. Abu-Nada, Z. Masoud, A. Hijazi: Natural convection heat transfer enhancement in horizontal concentric annuli using nanofluids, International Communications in Heat and Mass Transfer 35(2008) 657 – 665.

[14] A. Bijan: Convection heat transfer, Willey, NewYork, Third edition (1984).

[15] K. Khanafer, K. Vafai: A critical synthesis of thermo physical characteristics of nanofluids, International Journal of Heat and Mass Transfer 54 (2011) 4410-4428.

[16] H.C. Brinkman: The viscosity of concentrated suspensions and solution, The Journal of Chemical Physics 20 (1952) 571–581.

[17] J. Maxwell: A Treatise on Electricity and Magnetism, second ed., Oxford University Press, Cambridge, UK (1904).

[18] J. Koo, C. Kleinstreuer: A new thermal conductivity model for nanofluids, Journal of Nanoparticle Research 6 (2004) 577–588.

[19] R.S. Vajjha, D.K. Das: Experimental determination of thermal conductivity of three nanofluids and development of new correlations, International Journal of Heat and Mass Transfer 52 (2009) 4675–4682.

[20] J. Li, C. Kleinstreuer: Thermal performance of nanofluid flow in microchannels, International Journal of Heat and Fluid Flow 29 (2008) 1221–1232.

[21] B. Xiao, Y. Yang, L. Chen: Developing a novel form of thermal conductivity of nanofluids with Brownian motion effect by means of fractal geometry, Powder Technology 23 (2013) 409–414.

[22] M. Hemmat Esfe, S. Saedodin, O. Mahian, S, Wongwises: Thermal conductivity of Al_2O_3/water nanofluids, Journal of Thermal Analysis and Calorimetry 117(2014) 675–681.